Chinese Journal of Polymer Science Vol. 32, No. 9, (2014), 1176−1187

Chinese Journal of Polymer Science

Formation of Poly(L-lactide) Mesophase and Its Chain Mobility Dependent Kinetics*

Yuan-ying Liang, Hu Tang, Gan-ji Zhong** and Zhong-ming Li**

College of Polymer Science and Engineering, State Key Laboratory of Polymer Materials Engineering, Sichuan University, Chengdu 610065, China

Abstract In the present work, the PLLA mesophase formation and its kinetics at the advent of a chain mobility accelerator (polyethylene glycol (PEG)) are investigated by wide angle X-ray diffraction (WAXD) and time-resolved Fourier transform infrared spectroscopy (FTIR). It is interestingly found that the presence of PEG could accelerate the formation of PLLA mesophase notably due to the enhanced chain mobility, giving rise to a substantially reduced half time ($t_{0.5}$) of PLLA mesophase formation from 129 min to 8 min. The Avrami exponents (n) for the kinetics of mesophase formation are ~0.5 for neat PLLA and 1 for PLLA/PEG, respectively, indicating that 1D-rod growth through heterogeneous nucleation occurs during formation of PLLA mesophase. Tensile testing demonstrates that PLLA mesophase could increase the tensile strength and modulus but decrease the elongation at break.

Keywords: Poly(L-lactide); Chain mobility; Mesophase; Kinetics.

Electronic Supplementary Material Supplementary material is available in the online version of this article at http://dx.doi.org/10.1007/s10118-014-1505-y.

INTRODUCTION

Poly(L-lactide) (PLLA), a biodegradable aliphatic polyester derived from renewable resources, has received increasing attention due to the well-balanced mechanical properties and processability which can match with petroleum-based commodity polymers such as polystyrene and polypropylene[1]. However, high brittleness and poor ductility restrict its substitution of petroleum-based commodity polymers. Therefore, considerable efforts have been made to improve its flexibility (or toughness) as well as comprehensive properties.

Plasticization is an effective method to substantially enhance polymer chain mobility, leading to the rise of elongation at break and the extension of the potentials of PLLA in applications of packaging and mulch. Various types of chain mobility accelerators are expected to be promising in improving the ductility of PLLA, especially the environment-friendly ones such as poly(ethylene glycol) (PEG)[2–4], poly(ethylene oxide)[5–6], oligomeric lactic acid[7], glycerol[8], citrate ester[9], triacetine[10], tributyl citrate[10], acetyltriethyl citrate[11], tributyl citrate

* This work was financially supported by the National Natural Science Foundation of China (Nos. 51120135002, 51203104), the Doctoral Program of the Ministry of Education of China (No. 20120181120101), the Program of Introducing Talents of Discipline to Universities (B13040), and the Innovation Team Program of Science & Technology Department of Sichuan Province (No. 2013TD0013).

** Corresponding authors: Gan-ji Zhong (钟淦基), E-mail: ganji.zhong@scu.edu.cn
Zhong-ming Li (李忠明), E-mail: zmli@scu.edu.cn

Invited paper for the special issue of "Polymer Crystallization"
Received March 18, 2014; Revised April 24, 2014; Accepted May 9, 2014
doi: 10.1007/s10118-014-1505-y

oligomers[12], diethyl bishydroxymethyl malonate oligomers[13], glucosemonoesters[14] and partial fatty acid ester[15].

The crystallization behavior of PLLA containing chain mobility accelerator is of practical importance because the crystal structure and morphology are directly related to the macroscopic properties of the resultant products[16]. Hitherto, a consistent conclusion has been well established that the addition of a chain mobility accelerator can decline the glass transition temperature (T_g) and facilitate the crystallization kinetics of PLLA[4, 15, 17]. A decreased T_g was observed in using various accelerators of chain mobility, such as citrate esters[18], oligomeric lactic acid[8] and PEG[19]. The acceleration of chain mobility was responsible for the increased crystallization temperature during non-isothermal crystallization and high crystallinity[20]. However, phase separation over time also could be triggered by the promoted crystallization behavior[4, 15, 20–23], especially when T_g decreases below the room temperature, which could cause the loss of high ductility. Recently, a stable phase structure was formed through chemical grafting of PEG *via in situ* reactive blending, which significantly decreased the T_g and expanded the glass transition temperature range, thus a desirably elongation at break was achieved[24].

It is well known that PLLA can form four crystal modifications, α, α', β and γ forms, which depend upon crystallization conditions, such as crystallization temperature[25, 26], flow field[27] *etc*. Recently, the mesophase of polymers, such as polyethylene terephthalate[28], polypropylene[29, 30] and PLLA, as an intermediate state between crystalline and amorphous states, have also intrigued great interests of researchers. Mulligan and Camak[31] reported the occurrence of a nematic-like ordered structure with the help of X-ray scattering and birefringence measurements upon drawing PLLA just above T_g. Very recently, by employing various techniques including X-ray diffraction, differential scanning calorimetry (DSC) and Fourier transform infrared spectroscopy (FTIR), Stoclet *et al*.[32, 33] observed the mesophase induced by drawing the amorphous state of PLLA over the temperature range from 45 °C to 90 °C. They proposed that the strain-induced PLLA mesophase appeared as far as the temperature lower than 70 °C. Zhang *et al*.[34] also identified the formation of mesophase in the PLLA domains of quenched PLLA-PEG-PLLA block copolymers and aged PLLA by means of FTIR, in which a characteristic band at 915 cm^{-1} was detected. Their very recent result showed that physical aging below the T_g of PLLA gave rise to the formation of mesophase due to the conformational and micro-structural rearrangements of PLLA chains[35].

Albeit the formation of PLLA mesophase was deciphered in the aforementioned systems, the complete understanding of the influence of chain mobility accelerator, such as PEG, on the formation of PLLA mesophase and the relationship between the PLLA mesophase and the mechanical properties of PLLA/PEG blends, however, remains a scientific challenge. In the current work, the formation of PLLA mesophase and its kinetics by incorporating a small amount of PEG (as a chain mobility promoter) are studied by wide angle X-ray diffraction (WAXD) and time-resolved FTIR, aiming at throwing some light on better understanding of PLLA mesophase. Furthermore, the effect of mesophase formation on the mechanical properties of PLLA has also been explored so as to establish the relationship between the microscopic structure and macroscopic properties of PLLA. It is found that the PEG chain significantly accelerates the formation of mesophase, and subsequently the formation of mesophase improves the mechanical properties of the PLLA product.

EXPERIMENTAL

Materials and Sample Preparation

Commercially available PLLA (4032D) was purchased from Nature Works (USA) with a stereoisomer composition of about 2% D-isomer lactide. The weight-average molecular weight and number-average molecular weight were 2.23×10^5 g/mol and 1.06×10^5 g/mol, respectively. PEG (trade name Carbowax) with a nominal weight-average molecular weight of 3350 g/mol and melting temperature of about 50 °C was supplied by Dow Chemical Company (USA). Dichloromethane (CH_2Cl_2, AR grade) was purchased from Chengdu Kelong Chemical Reagent Factory (Chengdu, China) and was used as received. An optimal ratio of PEG and

PLLA by weight (20:80) was chosen in this paper (See SI-1), and they were dissolved in CH_2Cl_2. Then the homogeneous solution was placed overnight at room temperature for the evaporation of solvent followed by drying in a vacuum oven at 40 °C for 48 h to remove residual solvent. The PEG plasticized PLLA sample was termed as PPLA for concision, and the neat PLLA was also prepared under the same process for comparison. The dried PLLA and PPLA samples were hot-pressed at a temperature of 200 °C for 2 min. The hot-pressed PLLA and PPLA samples were subsequently quenched in liquid nitrogen. The aged PPLA sample was obtained through annealing the quenched sample in a vacuum oven at 53 °C for 1 h. The samples for WAXD measurements and tensile tests had a thickness of 0.3 mm and the samples for FTIR characterization had a thickness of 20 μm. For tensile testing, the samples were cut into dumbbell specimens with 4 mm in width and 20 mm in length.

Characterization

Wide angle X-ray diffraction

WAXD measurements were performed on the U7B beamline at the National Synchrotron Radiation Laboratory, Hefei, China (wavelength λ = 0.14809 nm). The WAXD patterns for both quenched and aged samples were collected by an X-ray CCD detector (Model Mar 345, MAR Research Co. Ltd., Germany).

Time-resolved FTIR characterization

To *in situ* trace the structural change of PPLA during aging, the time-resolved FTIR measurements were performed on a Nicolet 6700 FTIR spectrometer (Thermal Scientific, USA) equipped with a parallel-plate cell as a hot stage (HT-32, accuracy of ± 1 K). The film of PPLA was sandwiched between two ZnSe plates so as to adopt the transmission mode over the wavenumber range of 650−4000 cm^{-1}. The spectra were obtained by averaging 16 scans at a resolution of 2 cm^{-1} with a regular interval. In the non-isothermal process, PEG was found to be totally melted at 53 °C. Therefore, in order to eliminate the effect of PEG spectra change on the PLLA spectra, the temperature of 53 °C was chosen to study the kinetics of mesophase formation in the aging process of PPLA. The quenched film of PPLA was first placed in the transmission cell which was preheated to 53 °C and the data collection started at the temperature of 53 °C until the completion of the mesophase formation process. Here, the intensity referred to the peak height of characteristic bands, and the baseline of each spectrum was linearly corrected according to the same standard.

Mechanical property testing of quenched and aged PPLA

Tensile properties were measured with the help of a Shimadzu AGS-J test machine at a cross-head speed of 10 mm/min at room temperature. Each value of mechanical properties reported was an average of five specimens. The Young's modulus *E* was obtained from the tangent of initial slope of the stress versus strain curve.

RESULTS AND DISCUSSION

Mesophase Formation in Aged PPLA Studied by WAXD and FTIR

Figure 1 shows 2D-WAXD patterns of the quenched PPLA and the aged PPLA at 53 °C for 1 h. No obvious diffraction rings for crystalline phase such as (200)/(110) and (203) reflections of α form of PLLA are observed in the pattern of quenched PPLA, which is similar to the 2D-WAXD pattern of typical amorphous PLLA[32]. However, an obvious diffraction ring with a certain width is observed in the pattern of aged PPLA. This means some kind of ordered structure, different from the crystalline phase, was formed in the aging process.

Figure 2 shows the azimuthal integration of the 2D patterns of Fig. 1, which is applied to get insight into the ordered structure in the aging process. As depicted in Fig. 2(a), the quenched PPLA displays a broad diffraction peak which could be fitted by two amorphous peaks around 15.0° and 21.2° with full-width at half-maximum (fwhm) of about 8°. Though the chain mobility of PLLA is enhanced by PEG, the large cooling rate allowed almost no ordered structure to develop. In contrast, the PPLA sample annealed at 120 °C exhibits the characteristics of typical crystalline PLLA, *i.e.* crystalline peaks at 14.8° (*i.e.* (010)), 16.7° (*i.e.* (200)/(110)),

19.1° (*i.e.* (203)), and 22.4° (*i.e.* (015)) with the fwhm of around 0.5°. Interestingly, different from typical amorphous and crystalline PLLA, the aged PPLA sample shows a diffraction peak with fwhm in the range between 0.5° and 8°. When the profile of aged PPLA is fitted by Gaussian equation, besides two amorphous peaks with fwhm of 8° at 2θ = 15.0° and 21.0°, another peak at 16.2° with the fwhm of 3.5° is needed (Fig. 2b), which was assigned to strain-induced mesophase of PLLA by Stoclet *et al*[32]. The higher value of 2θ (16.2°) with respect to the main amorphous halo (15.0°), indicates that the average inter-chain distance is substantially reduced compared to the spacing of the amorphous chains. Therefore, the ordered structure formed in aged PPLA might also be a kind of mesophase and possibly has the same nature as the strain-induced mesophase.

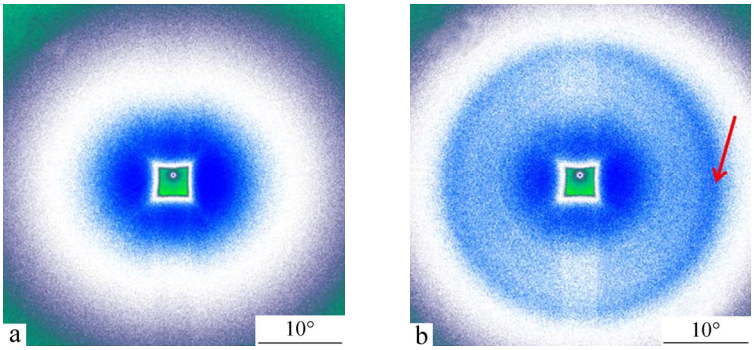

Fig. 1 2D wide angle X-ray diffraction patterns of (a) quenched and (b) aged PPLA (The 2θ-scale bar is inserted.)

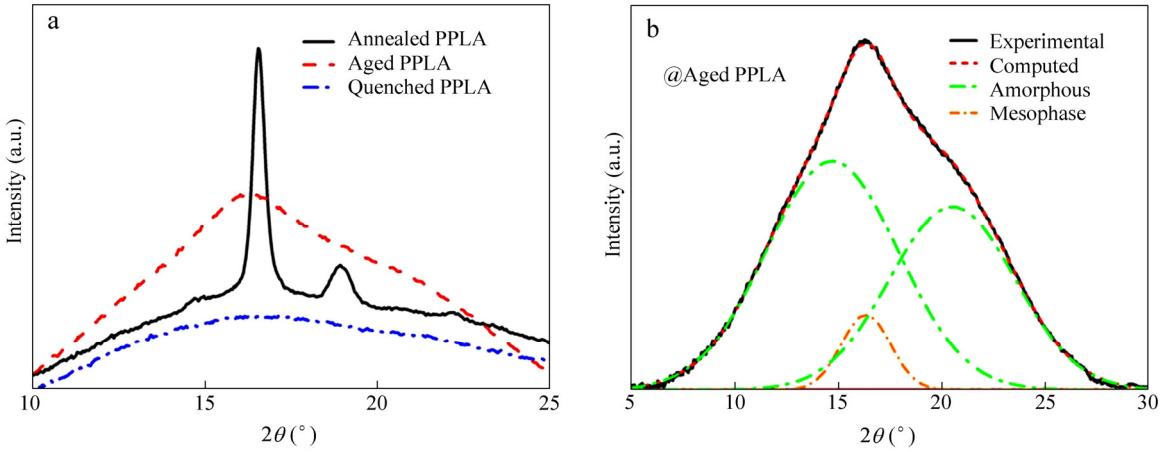

Fig. 2 (a) Azimuth-integrated WAXD intensity profile of quenched and aged PPLA (1D-WAXD profile of PPLA annealed at 120 °C for 1 h is also presented for comparison), and (b) the curve fitting analysis of the WAXD intensity profile of aged PPLA

To further check the feature of ordered structure formed in the aged PPLA, FTIR was employed to investigate the local structure of PLLA chains, since the solid phase structure is directly related to local molecular structure such as molecular conformation[36]. The time-resolved FTIR measurement of PEG is performed to eliminate the effect of PEG phase behavior on the PLLA spectrum. As depicted in Fig. 3, there are sharp characteristic bands of PEG crystals at the location of 2883 cm^{-1}, 1116 cm^{-1}, 842 cm^{-1}, 946 cm^{-1}, 1061 cm^{-1}, 1149 cm^{-1}, 1281 cm^{-1}, 1360 cm^{-1} and 1468 cm^{-1}. As temperature increases, PEG crystals gradually melt and the intensity of those bands decreases, accompanying with the shift of the wavenumber. PEG crystals totally melt at the temperature of 53 °C. As a result, 2879 cm^{-1} shifts to 2867 cm^{-1}, 1118 cm^{-1} shifts to 1111 cm^{-1}, and the other bands disappear. From 53 °C to 80 °C, the FTIR spectrum keeps unchanged,

demonstrating that PEG keeps in liquid state during the whole temperature range. Therefore, 53 °C is chosen as the aging temperature of PPLA as PEG stays in the molten form and its spectrum stays unchanged at this temperature.

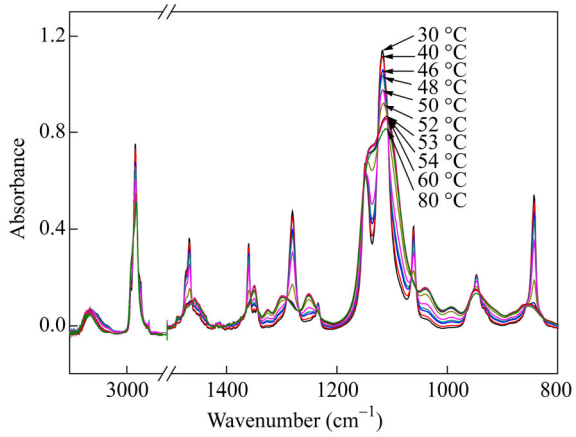

Fig. 3 IR spectra evolution of PEG during the heating process from 30 °C to 80 °C with the heating rate of 1 K/min

Figure 4 illustrates the comparison of the FTIR spectra between the quenched and aged PPLA. FTIR spectrum of the quenched PLLA is also presented for comparison in Fig. 4(a). At the first glance, almost no difference between quenched PLLA and PPLA is observed, except for a small band at 2883 cm^{-1} which is assigned to CH_2 stretching vibration of PEG chains. However, it can be observed in Fig. 4(b) that a band in C=O stretching vibration region (1800–1720 cm^{-1}) is located at 1757 cm^{-1} for quenched PPLA while it is shifted to 1755 cm^{-1} for aged PPLA. It was reported by Zhang *et al.*[26, 37] that typical FTIR bands in the C=O stretching region for amorphous, α' and α forms of PLLA were located at 1757, 1761, and 1759/1749 cm^{-1}, respectively. Thus, the quenched PLLA is mainly in their amorphous state, which is consistent with the results of WAXD (Fig. 2a). In contrast, the aged PPLA displays the wavenumber shift of the amorphous band from 1757 cm^{-1} to 1755 cm^{-1}. Since the band at 1755 cm^{-1} is not the characteristic band of either α' or α form, and a higher shift from 1757 cm^{-1} to 1753 cm^{-1} was also proposed by Zhang *et al.*[34] for PLLA mesophase in quenched PLLA-PEG-PLLA copolymer. As a consequence, it is believed that the band at 1755 cm^{-1} could stem from mesophase formed in PLLA homopolymer[34]. According to Meaurio *et al.*, the larger shift of 1757 cm^{-1} might be attributed to an increase of the relative population of *tt* conformers accompanying with the mesophase formation[38]. The assumption is further verified by the intensity change of band at 1267 cm^{-1} between quenched and aged PPLA, which is associated with the coupling of υ_{as}(C−O−C) and δ(CH) vibration modes and also sensitive to the amorphous phase of PLLA (see Fig. 4c). The intensity of band at 1267 cm^{-1} drops after aging in our sample, suggesting the depletion of amorphous phase of PLLA during the aging process, *i.e.* some ordered structure is forming. Moreover, the further valid evidence is provided by spectrum comparison in the chain backbone vibration region (970–830 cm^{-1}) of PLLA. The quenched PPLA shows almost no band around 921 cm^{-1} (Fig. 4d). Note that, the 921 cm^{-1} band is assigned to the 10_3 helix conformation of α or α' form[39–42] and the 908 cm^{-1} band is assigned to 3_1 helix of β form[43, 44], suggesting little or no crystalline structure is generated in the quenching process. Clearly, the aged PPLA exhibits a band at 915 cm^{-1}, which is in agreement with the observation of mesophase formed by quenching PLLA-PEG-PLLA copolymer[34].

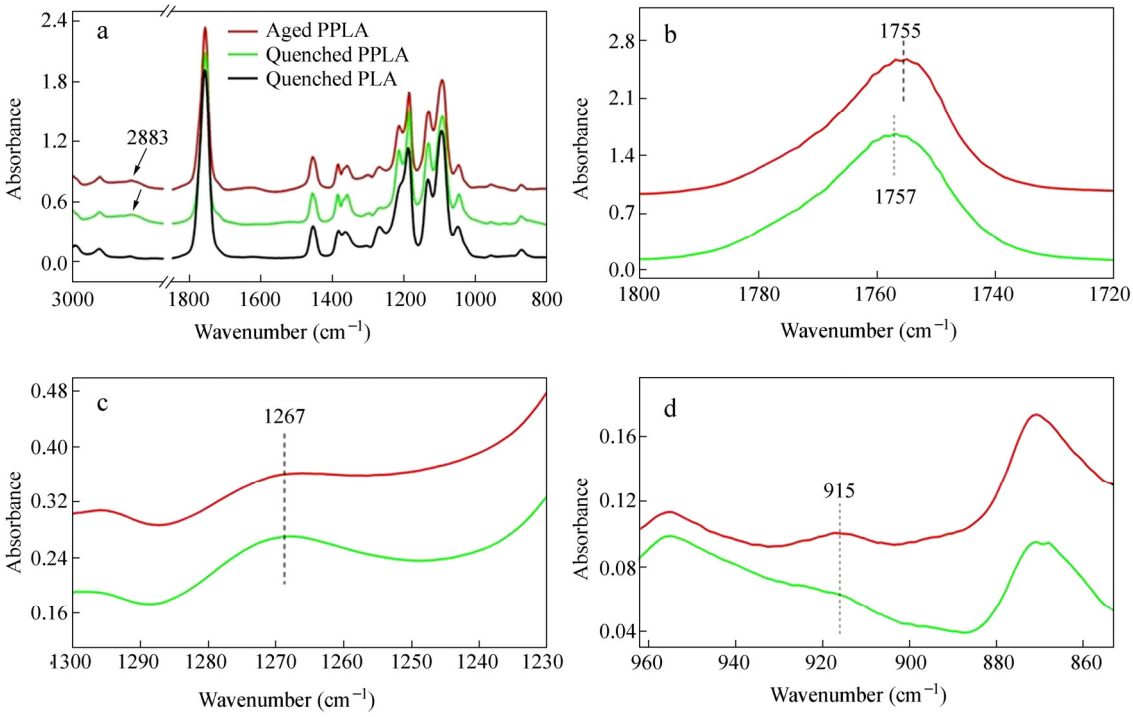

Fig. 4 Comparison of FTIR spectra between quenched PPLA and aged PPLA in the wavenumber range of (a) 3100–800 cm^{-1}, (b) 1800–1720 cm^{-1}, (c) 1300–1230 cm^{-1} and (d) 970–835 cm^{-1} (FTIR spectrum of quenched PLLA is also presented for comparison in (a).)

Combining the WAXD results with the FTIR ones, it can be concluded that mesophase is definitely formed in the aged PPLA[35], where the PLLA mesophase shares the same characteristics in the terms of configuration (*i.e.* helix configuration) with strain-induced mesophase in PLLA[33] and quench-induced mesophase in PLLA-PEG-PLLA copolymer[34]. This result gives rise to a hint that the PLLA mesophase is a kind of thermodynamically stable ordered structure like α, β and γ forms of PLLA in the viewpoint of thermodynamics (See SI-2). Taking glass transition temperature (about 60 °C) of PLLA into consideration, the formation of PLLA mesophase in neat PLLA is unfavorable in terms of kinetics. It is also reported that the melting temperature of mesophase is around 70 °C and mesophase could only form under about 70 °C[32]. Therefore, the stress exerted in strain-induced mesophase in PLLA or the introduction of PEG molecules in PLLA-PEG-PLLA copolymer or the aging treatment to PPLA is to enhance kinetics of mesophase formation. In this work, the addition of 20 wt% PEG in PLLA could remarkably improve the chain mobility, thus the kinetics of mesophase formation could be altered, which will be discussed below.

Mesophase Formation in PPLA in the Aging Process Studied by in-situ FTIR

As confirmed by WAXD and FTIR, nearly no ordered structure is generated in PPLA during the quenching process while mesophase forms in the course of aging. *In situ* FTIR experiments of PPLA are carried out to investigate the formation kinetics of mesophase at 53 °C, as shown in Fig. 5. With the extension of aging time, the formation of mesophase in PPLA is evident by the change of characteristic FTIR bands. That is, the band at 1757 cm^{-1} turns to 1755 cm^{-1} (Figs. 5a and 5b), the intensity of the band at 1267 cm^{-1} for amorphous phase decreases (Figs. 5a and 5d), and the intensity at 915 cm^{-1} increases (Fig. 5c). These results are strongly responsible for the development of mesophase in PPLA during the aging process[34]. The variation of wavenumber in the 1800–1720 cm^{-1} region and the intensity changes at 1267 cm^{-1} as well as 915 cm^{-1} for PPLA during the aging process are illustrated in Fig. 6. The changes in all the three regions are in accordance with the same law (almost at the same speed) as the aging time increases and reach to the platform in about 30 min,

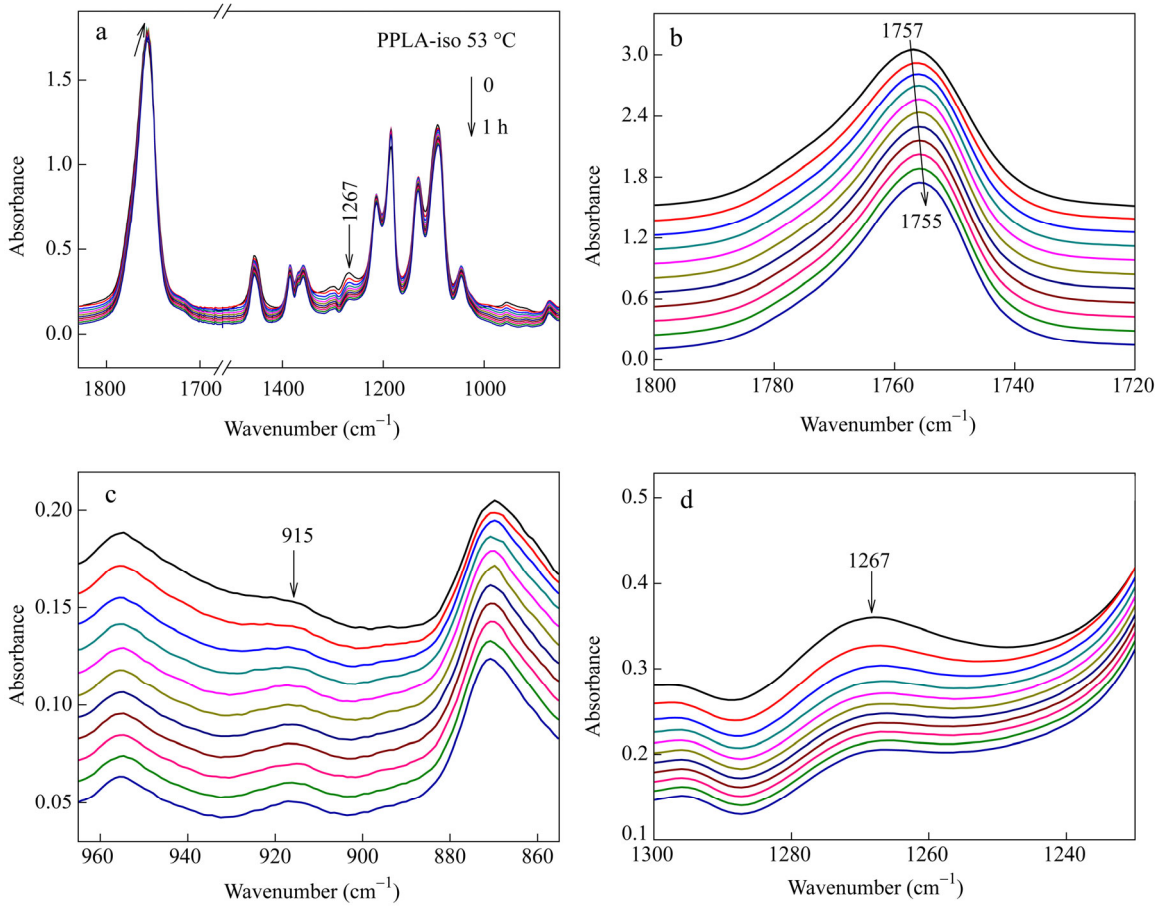

Fig. 5 FTIR spectra evolution of PPLA during the aging process at 53 °C for 1 h in the region of (a)1800–800 cm^{-1}, (b)1800–1720 cm^{-1}, (c) 1300–1230 cm^{-1} and (d) 970–850 cm^{-1}

indicating the completion of mesophase formation in PPLA while aging at 53 °C. Of particular note, the evolution of these characteristic bands as a function of time does not satisfy the typical "S" shape curve since mesophase actually exists in the quenched PLLA notwithstanding its content is hard to be detected by the WAXD technique. In fact, according to Zhang *et al.*, 3% mesophase already existed in quenched PLLA[34]. The PLLA chain mobility in PPLA could be enhanced due to the existence of PEG, so it is reasonable to conjecture that a certain amount of mesophase should be obtained in the aged PPLA.

As aforementioned, mesophase is a kind of ordered structure different from typical crystalline PLLA. To evaluate the growth dimension of mesophase, the well-known Avrami equation is usually employed and its linear form is given as follows[45],

$$\ln\left\{-\ln\left[1-X(t)\right]\right\} = \ln k(t) + n\ln t \tag{1}$$

where $X(t)$ is the relative crystallinity at a given time t, k is the crystallization rate constant, and n is the Avrami exponent, which is typically related to the nature of nucleation and to the growth dimension of polymers[35]. In addition, given that n and k are calculated by equation (1), $t_{0.5}$ which refers to the time when half of the crystallization is done can be calculated by $t_{0.5} = \left[\ln 2 / k\right]^{1/n}$.

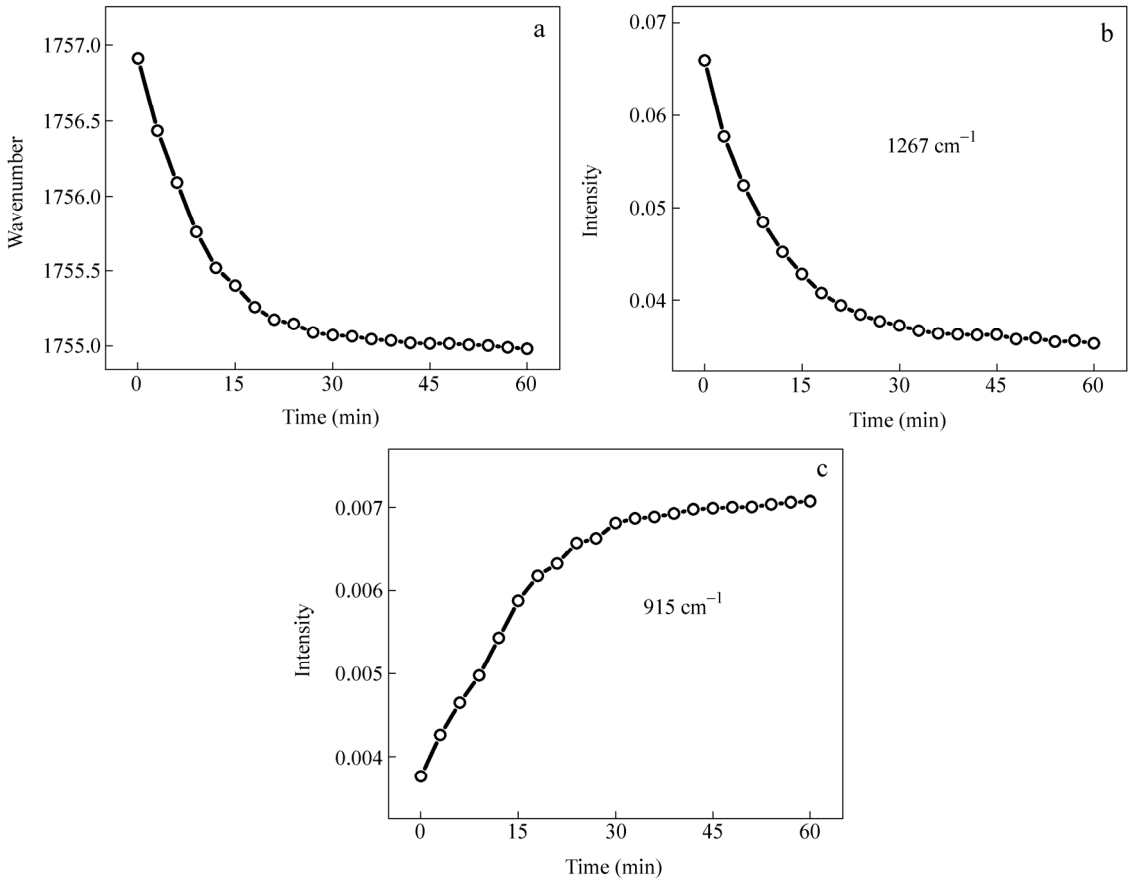

Fig. 6 (a) The wavenumber changes in the 1800–1720 cm^{-1} region, the intensity changes at (b) 1267 cm^{-1} and (c) 915 cm^{-1} for PPLA during the aging process

Here the relative crystallinity is calculated by $X_t = (I_t - I_\infty)/(I_0 - I_\infty)$, where I_t is the peak intensity at the aging time t, I_0 and I_∞ are the initial and final peak intensities in the whole aging process respectively. Equation (2) which is often used to study the crystallization dynamics by spectrum techniques is obtained.

$$\ln\{-\ln[(I_t - I_\infty)/(I_0 - I_\infty)]\} = \ln k(t) + n \ln t \tag{2}$$

In order to study the kinetics of mesophase formation, the band at 1267 cm^{-1} is examined because the intensity changes of this band is more obvious and less error would be caused during the fitting process. As illustrated in Fig. 7, the relationship between $\ln\{-\ln[(I_t - I_\infty)/(I_0 - I_\infty)]\}$ and ln$t$ during the isothermal process is well linearly fitted, implying the rationality of using Avrami equation to fit the mesophase formation process. For comparison, the mesophase formation of PLLA aged at 53 °C for 24 h is also investigated, as shown in Fig. 8. Unlike Zhang's study[34], there are no obvious spectra changes in the region of 1800–1720 cm^{-1} and 970–850 cm^{-1}. This might be ascribed to the poorer chain mobility of PLLA used in our case stemming from the higher molecular weight. While by examining the 1200–1300 cm^{-1} region, the intensity of band at 1267 cm^{-1}, which is sensitive to amorphous phase of PLLA, decreases gradually with the aging time (Fig. 8b). It is worth noting that $t_{0.5}$ for mesophase formation at 53 °C is only 8.4 min for PPLA, which is much less than that for neat PLLA with the $t_{0.5}$ equaling to 129 min (Fig. 8b). This verifies that the ability of mesophase formation is remarkably improved by the enhanced chain mobility of PLLA in PPLA.

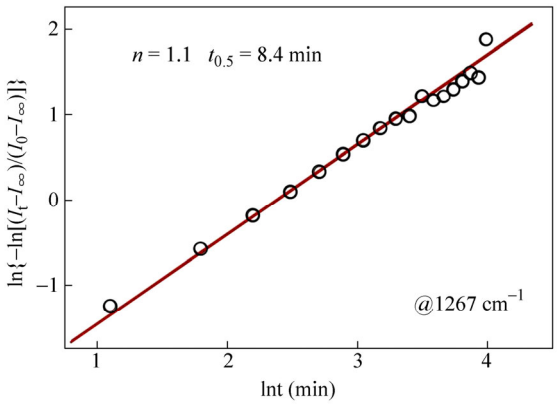

Fig. 7 Curve fitting results on the growth of mesophase of aged PPLA using the intensity change at 1267 cm^{-1} during the aging process at 53 °C for 1 h

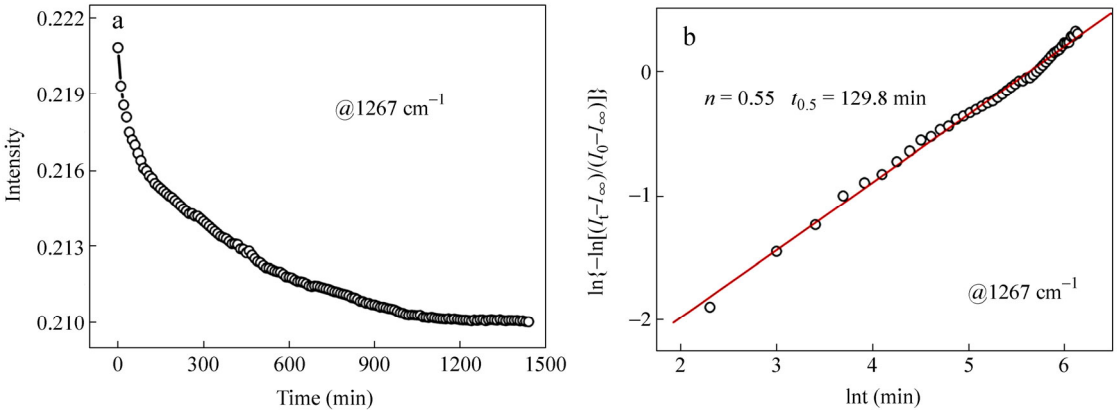

Fig. 8 (a) Intensity change of PLLA at 1267 cm^{-1} and (b) the curve fitting results on the growth of mesophase using the intensity change at 1267 cm^{-1} during the aging process

The structure of mesophase in PPLA and PLLA might be deciphered by analyzing n. The n of mesophase formation at 53 °C is about 1 for PPLA and 0.55 for PLLA. The value of n for neat PLLA is in agreement with Zhang's study[35] in which the n was around 0.4–0.5 by analyzing the intensity changes of bands at 918 cm^{-1} and 956 cm^{-1}. For PLLA crystallization in a large range of temperature, *i.e.* from 80 to 140 °C, n values varied in the range of 2.0 to 5.4 have been reported[46–48] which could be affected by many factors such as athermal nucleation or thermal nucleation, volume change during changing of nucleation mechanism during crystallization. But none of these values is low enough to 0.5 and 1 as in this work. This observation suggests that the formation kinetics of the local ordered structure, which is less ordered than that of a three-dimensional ordered crystal, is totally different from the crystallization process. According to classic crystallization theory, the n is composed of two terms:

$$n = n_d + n_n \tag{3}$$

where n_d represents the dimensionality of the growing crystals and this quantity can only have, as values, the integer numbers 1, 2, 3, corresponding to one, two, three-dimensional entities. The time dependence of the nucleation is represented by n_n. In principle, the value of n_n should be either 0 or 1, where 0 corresponds to instantaneous or heterogeneous nucleation and 1 to sporadic or homogenous nucleation. Considering the relatively low value of n in this work, n_n should be 0, *i.e.* the nucleation mechanism of mesophase formation should be heterogeneous nucleation. The n around 1 for mesophase formation in PPLA indicates that the

mesophase in PPLA grows into 1D rods rather than 3D spherulites. The deduction was also verified by pioneer work on the PLLA crystallization under CO_2 with high pressure at low temperature by Marubayashi[49]. It proposed that PLLA developed into 1D rods in the low temperature ranging from 20 °C to 60 °C, which should also be a kind of mesophase. The lower *n* value of neat PLLA might be ascribed to the lower dimension of PLLA mesophase developed in this system, *i.e.* some mesophase of 0D points together with 1D rods are developed in neat PLLA due to its intrinsic low chain mobility.

Mechanical Properties of PLLA Mesophase in PEG Plasticized PLLA

The results of WAXD and FTIR identify the formation of PLLA mesophase in aged PLLA and PPLA. As the microstructure of polymer is directly relevant to its macroscopic performance, thus the presence of mesophase stimulates our curiousness to investigate the relationship between mesophase and mechanical properties. The stress-strain curves of quenched and aged PPLA are depicted in Fig. 9. Clearly, the formation of mesophase in aged PPLA decreases its elongation at break slightly (from 9.8% to 7.8%) but raises its yield strength (from 30.6 MPa to 34.8 MPa) and tensile modulus (from 872.3 MPa to 1071.5 MPa). WAXD results indicate that PLLA mesophase formed in PPLA is a cohesive phase with shorter inter-chain distance compared with amorphous phase. Stoclet *et al.* reported strain-induced mesophase was also a cohesive phase which was responsible for the strain hardening behavior[32]. However, hitherto, no direct relationship between PLLA mesophase and its properties has been reported. In this work, for PPLA, the formation of PLLA mesophase could increase both strength and modulus whereas decrease its strain at break, which could be considered to play a positive stimulating role in tuning its properties and expanding the application of PLLA-based materials.

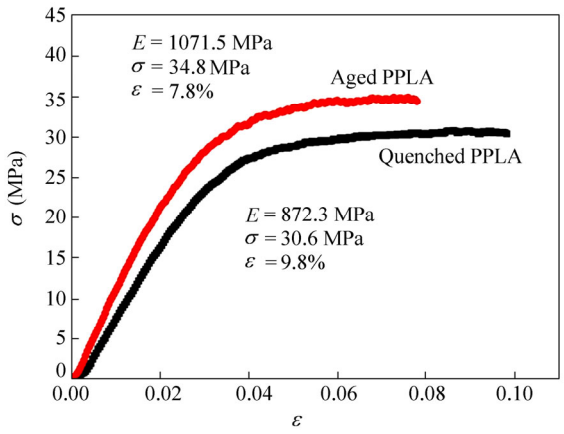

Fig. 9 Tensile stress-strain curves of quenched and aged PPLA

CONCLUSIONS

The PLLA mesophase formation in PEG plasticized PLLA was observed in this study. WAXD and FTIR confirmed the formation of mesophase during the aging process, and suggested that the mesophase obtained under different conditions might have the same nature. That is, the mesophase was an intrinsic ordered phase formed under low temperatures for PLLA as a counterpart of crystal in higher temperature region. The exertion of stress or introduction of PEG only enhanced its formation kinetics. *In situ* FTIR showed that mesophase formation kinetics was indeed dramatically enhanced by the addition of PEG through enhancing its chain mobility. Analysis of Avrami exponent *n* indicated that PLLA mesophase might be 1D rods grown through heterogeneous nucleation. Tensile testing demonstrated that PLLA mesophase as a cohesive phase would increase the tensile strength and modulus but decrease the elongation at break for plasticized PLLA.

ACKNOWLEDGEMENTS The authors are grateful to the National Synchrotron Radiation Laboratory (Hefei, China) and the beamline BL15U1 and BL16B1 of Shanghai Synchrotron Radiation Facility (SSRF, Shanghai, China) for the help with synchrotron X-ray scattering measurements.

REFERENCES

1 Gruber, P.R., Hall, E.S., Kolstad, J.J., Iwen, M.L., Benson, R.D. and Borchardt, R.L., Continuous process for the manufacture of lactide and lactide polymers. Google Patents: 2001
2 Sheth, M., Kumar, R.A., Davé, V., Gross, R.A. and McCarthy, S.P., J. Appl. Polym. Sci., 1997, 66: 1495
3 Yang, J.M., Chen, H.L., You, J.W. and Hwang, J.C., Polym. J., 1997, 29: 657
4 Younes, H. and Cohn, D., Eur. Polym. J., 1988, 24: 765
5 Nijenhuis, A., Colstee, E., Grijpma, D. and Pennings, A., Polymer, 1996, 37: 5849
6 Nakaruku, C., Polym. J., 1996, 28: 568
7 Sinclair, R., J. Macromol. Sci. A., 1996, 33: 585
8 Martin, O. and Averous, L., Polymer, 2001, 42: 6209
9 Labrecque, L., Kumar, R., Dave, V., Gross, R. and McCarthy, S., J. Appl. Polym. Sci., 1997, 66: 1507
10 Ljungberg, N., Andersson, T. and Wesslén, B., J. Appl. Polym. Sci., 2003, 88: 3239
11 Zhang, J.F. and Sun, X., Macromol. Biosci., 2004, 4: 1053
12 Ljungberg, N. and Wesslen, B., Polymer, 2003, 44: 7679
13 Ljungberg, N. and Wesslén, B., J. Appl. Polym. Sci., 2004, 94: 2140
14 Madhavan Nampoothiri, K., Nair, N.R. and John, R.P., Biores. technol., 2010, 101: 8493
15 Jacobsen, S. and Fritz, H.G., Polym. Eng. Sci., 1999, 39: 1303
16 Cheng, S., Chen, X., Hsuan, Y.G. and Li, C.Y., Macromolecules, 2011, 45: 993
17 Zhang, Y., Wang, Z., Jiang, F., Bai, J. and Wang, Z., Soft Matter, 2013, 9: 5771
18 Ljungberg, N. and Wesslén, B., Biomacromolecules, 2005, 6: 1789
19 Hu, Y., Hu, Y., Topolkaraev, V., Hiltner, A. and Baer, E., Polymer, 2003, 44: 5681
20 Hu, Y., Rogunova, M., Topolkaraev, V., Hiltner, A. and Baer, E., Polymer, 2003, 44: 5701
21 Ljungberg, N. and Wesslen, B., J. Appl. Polym. Sci., 2002, 86: 1227
22 Hu, Y., Hu, Y., Topolkaraev, V., Hiltner, A. and Baer, E., Polymer, 2003, 44: 5711
23 Ljungberg, N., Andersson, T. and Wesslén, B., J. Appl. Polym. Sci., 2003, 88: 3239
24 Choi, K.M., Choi, M.C., Han, D.H., Park, T.S. and Ha, C.S., Eur. Polym. J., 2013, 49: 2356
25 De Santis, P. and Kovacs, A.J., Biopolymers, 1968, 6: 299
26 Zhang, J., Duan, Y., Sato, H., Tsuji, H., Noda, I., Yan, S. and Ozaki, Y., Macromolecules, 2005, 38: 8012
27 Hoogsteen, W., Postema, A., Pennings, A., Ten Brinke, G. and Zugenmaier, P., Macromolecules, 1990, 23: 634
28 Ran, S., Wang, Z., Burger, C., Chu, B. and Hsiao, B.S., Macromolecules, 2002, 35: 10102
29 Wang, Z.G., Hsiao, B.S., Srinivas, S., Brown, G.M., Tsou, A.H., Cheng, S.Z. and Stein, R.S., Polymer, 2001, 42: 7561
30 Qiu, J., Wang, Z., Yang, L., Zhao, J., Niu, Y. and Hsiao, B.S., Polymer, 2007, 48: 6934
31 Mulligan, J. and Cakmak, M., Macromolecules, 2005, 38: 2333
32 Stoclet, G., Seguela, R., Lefebvre, J., Elkoun, S. and Vanmansart, C., Macromolecules, 2010, 43: 1488
33 Stoclet, G., Seguela, R., Lefebvre, J. M. and Rochas, C., Macromolecules, 2010, 43: 7228
34 Zhang, J., Duan, Y., Domb, A. J. and Ozaki, Y., Macromolecules, 2010, 43: 4240
35 Zhang, T., Hu, J., Duan, Y., Pi, F. and Zhang, J., J. Phys. Chem. B., 2011, 115: 13835
36 Zhang, J., Tsuji, H., Noda, I. and Ozaki, Y., J. Phys. Chem. B., 2004, 108: 11514
37 Zhang, J., Tsuji, H., Noda, I. and Ozaki, Y., Macromolecules, 2004, 37: 6433
38 Meaurio, E., Zuza, E., Lopez-Rodriguez, N. and Sarasua, J., J. Phys. Chem. B., 2006, 110: 5790
39 Kister, G., Cassanas, G. and Vert, M., Polymer, 1998, 39: 267
40 Kang, S., Hsu, S.L., Stidham, H.D., Smith, P.B., Leugers, M.A. and Yang, X., Macromolecules, 2001, 34: 4542
41 Meaurio, E., López-Rodríguez, N. and Sarasua, J., Macromolecules, 2006, 39: 9291

42 Pan, P., Zhu, B., Dong, T., Yazawa, K., Shimizu, T., Tansho, M. and Inoue, Y., J. Chem. Phys., 2008, 129: 184902
43 Sawai, D., Takahashi, K., Sasashige, A., Kanamoto, T. and Hyon, S.H., Macromolecules, 2003, 36: 3601
44 Lee, J.K., Lee, K.H. and Jin, B.S., Eur. Polym. J., 2001, 37: 907
45 Avrami, M., J. Chem. Phys., 1939, 7: 1103
46 Iannace, S. and Nicolais, L., J. Appl. Polym. Sci., 1997, 64: 911
47 Miyata, T. and Masuko, T., Polymer, 1998, 39: 5515
48 Kolstad, J.J., J. Appl. Polym. Sci., 1996, 62: 1079
49 Marubayashi, H., Akaishi, S., Akasaka, S., Asai, S. and Sumita, M., Macromolecules, 2008, 41: 9192